Electronic Supplementary Information

Nitrogen doped graphene anchored with mixed growth patterns of CuPt alloy nanoparticles as a highly efficient and durable electrocatalyst for oxygen reduction reaction in alkaline medium

Rajith Illathvalappil,[a,b] Vishal M. Dhavale,[a,b,‡] Siddheshwar N. Bhange[a,b,‡] and Sreekumar Kurungot*

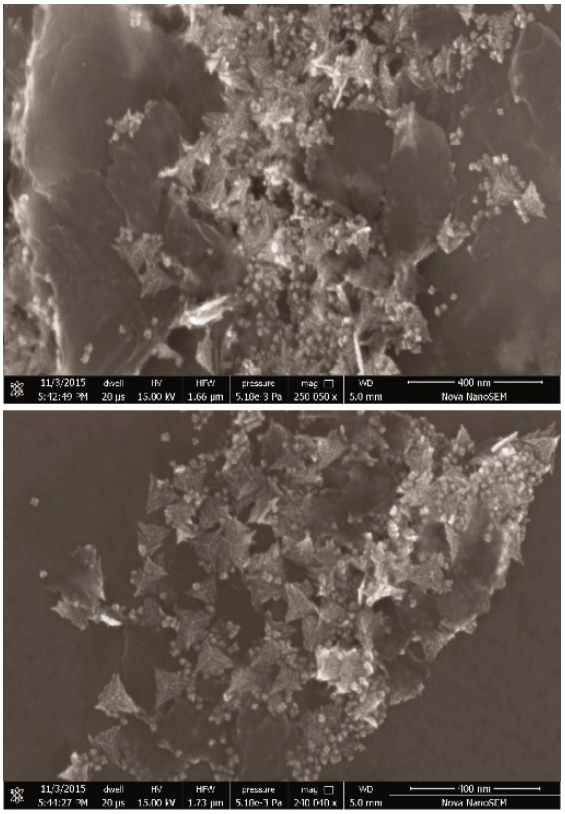

Fig. S1. *FESEM images of CuPt-TBTC/NGr-90.*

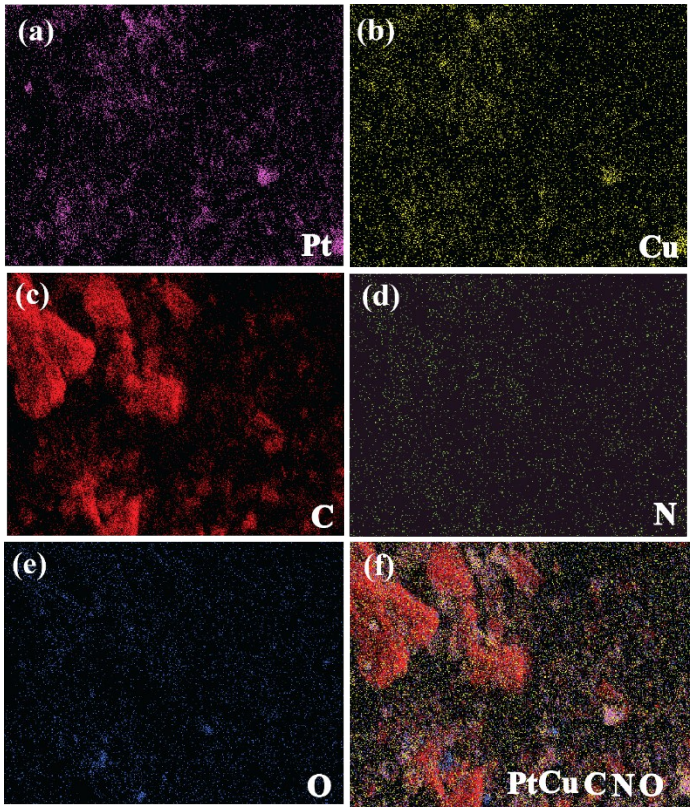

Fig. S2. *FESEM elemental mapping images of CuPt-TBTC/NGr-90: (a) platinum, (b) copper, (c) carbon, (d) nitrogen, (e) oxygen and (f) combined.*

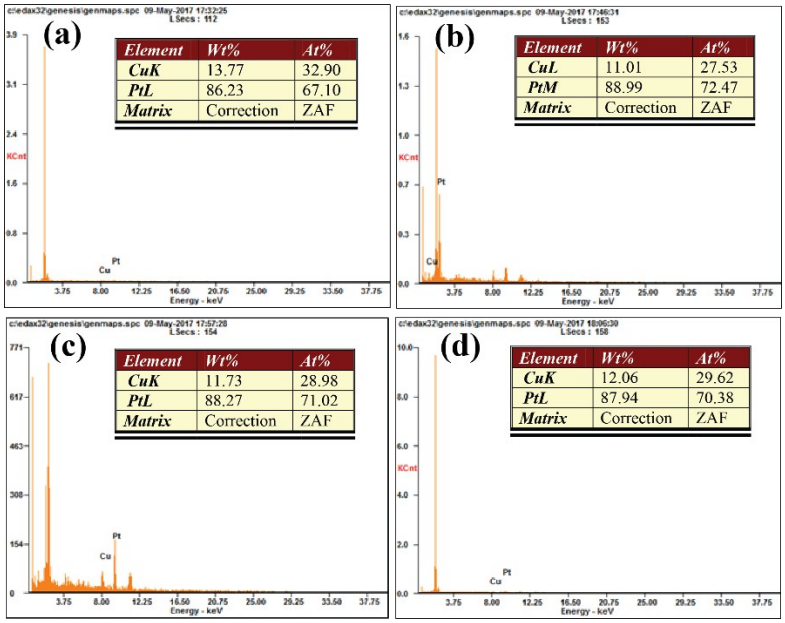

Fig. S3. *SEM-EDX analysis: a) CuPt-TBTC/NGr-30, b) CuPt-TBTC/NGr-60, c) CuPt-TBTC/NGr-90 and d) CuPt-TBTC/NGr-120.*

***Table S1**. Comparison of the elemental composition of the samples synthesized at different time interval using SEM-EDX analysis.*

Sample	Atomic % (Cu)	Atomic % (Pt)	Pt/Cu ratio
CuPt-TBTC/NGr-30	32.90	67.10	2.04
CuPt-TBTC/NGr-60	27.53	72.47	2.63
CuPt-TBTC/NGr-90	28.98	71.02	2.45
CuPt-TBTC/NGr-120	29.62	70.38	2.38

***Table S2**. Comparison of the elemental composition of the samples synthesized at different time interval using ICP analysis.*

Sample	Pt/Cu ratio
CuPt-TBTC/NGr-30	3.04
CuPt-TBTC/NGr-60	3.28
CuPt-TBTC/NGr-90	2.91
CuPt-TBTC/NGr-120	2.95

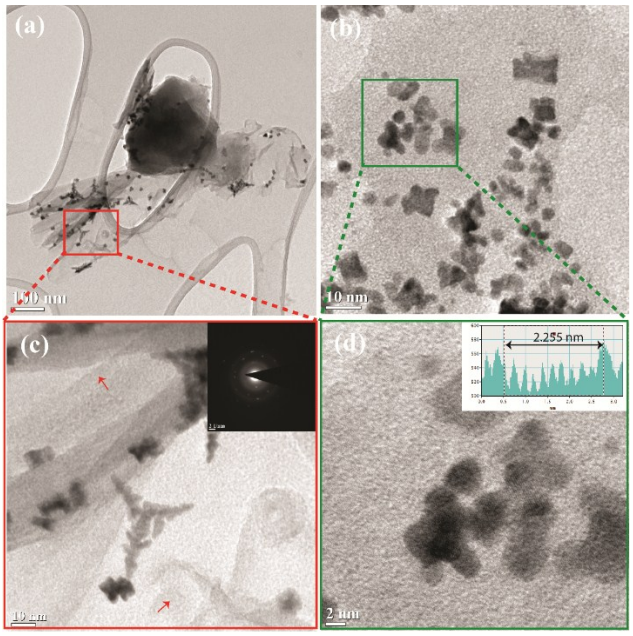

***Fig. S4.** TEM images of CuPt-TBTC/NGr-30 recorded at different magnifications: (a) image indicating the mixed dispersion of the tetrapod and disordered CuPt alloy particles on the surface of NGr, (b) higher magnification image of the disordered CuPt alloy particles, (c) magnified view of the tetrapod structures of the CuPt-alloy marked in the red square in (a) with the SAED pattern in the inset and the red arrows indicating the NGr support, and (d) higher magnification image of the disordered CuPt alloy particles marked in the green square in (b) with the inset showing the line profile of the CuPt alloy.*

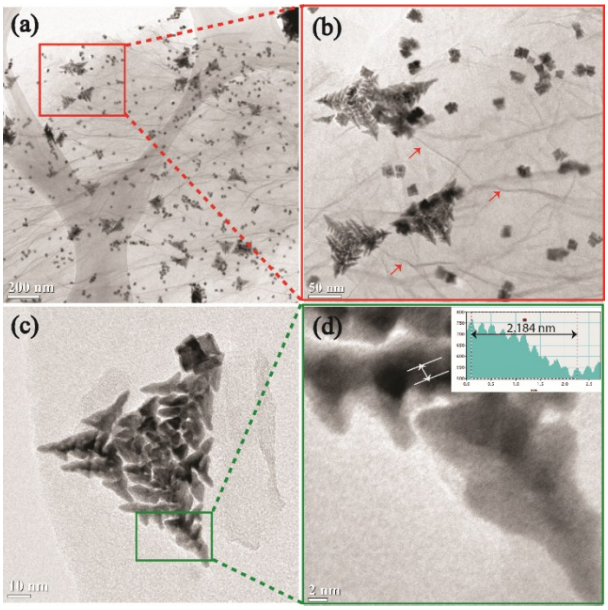

Fig. S5. *TEM images of CuPt-TBTC/NGr-60 recorded at different magnifications: (a) image indicating the mixed dispersion of the partially formed trigonal bipyramidal and truncated cubes on the surface of NGr, (b) higher magnification image of the marked (red) portion of (a) and the red arrows indicating the NGr support, (c) magnified image of the partially formed trigonal bipyramidal of the CuPt-alloy, and (d) magnified view of the region marked in the green square in (c) with the inset showing the line profile of the CuPt alloy.*

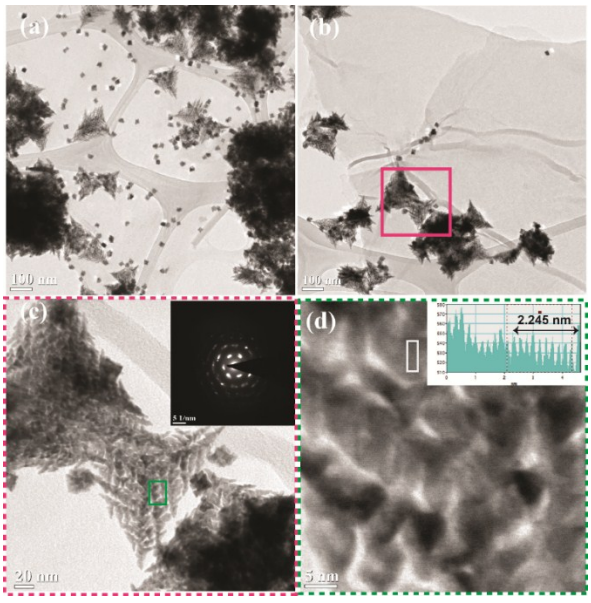

Fig. S6. *TEM images of CuPt-TBTC/NGr-120 recorded at different magnifications: (a) image indicating the agglomeration of the trigonal bipyramidal and truncated cubes on the surface of NGr, (b) higher magnification image of the agglomerated trigonal bipyramidal, (c) higher magnification image of the marked (red) portion of (b) with the SAED pattern in the inset, and (d) magnified view of the*

agglomerated trigonal bipyramidal marked in the green square in (c) with the inset showing the line profile of the CuPt alloy.

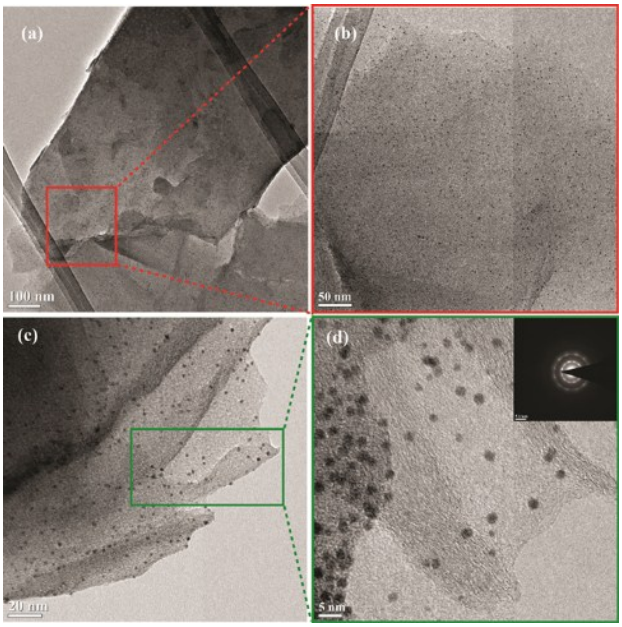

Fig. S7. *TEM images of CuPt/NGr-90 without KI addition at different magnifications: (a) image indicating the spherical particles on the surface of NGr, (b) higher magnification image of the marked (red) portion of (a), (c) magnified image of the spherical nanoparticle on NGr, and (d) magnified view of the spherical nanoparticle marked in the green square in (c) with the inset showing the SAED pattern.*

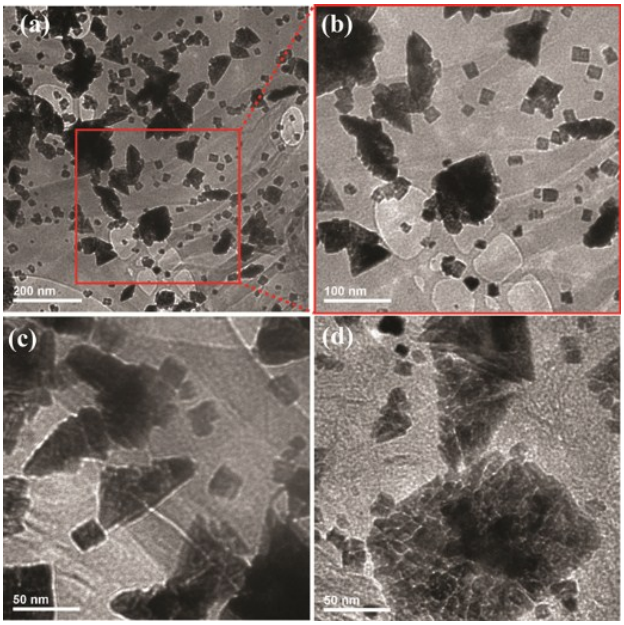

Fig. S8. *TEM images of CuPt/NGr-90 without PVP addition at different magnifications: (a) image indicating the agglomerated particles without proper geometry on the surface of NGr, (b) higher*

magnification image of the marked (red) portion of (a), (c) and (d) higher magnified image of the agglomerated particle on NGr.

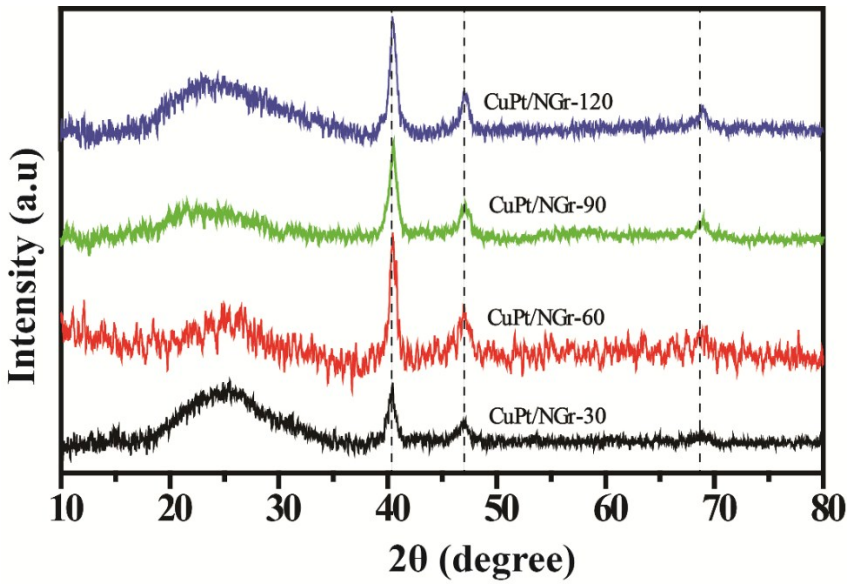

Fig. S9. *Comparative XRD patterns of CuPt/NGr-xx (where xx stands for 30, 60, 90 and 120 minutes of the reaction time intervals) recorded at different reaction time intervals.*

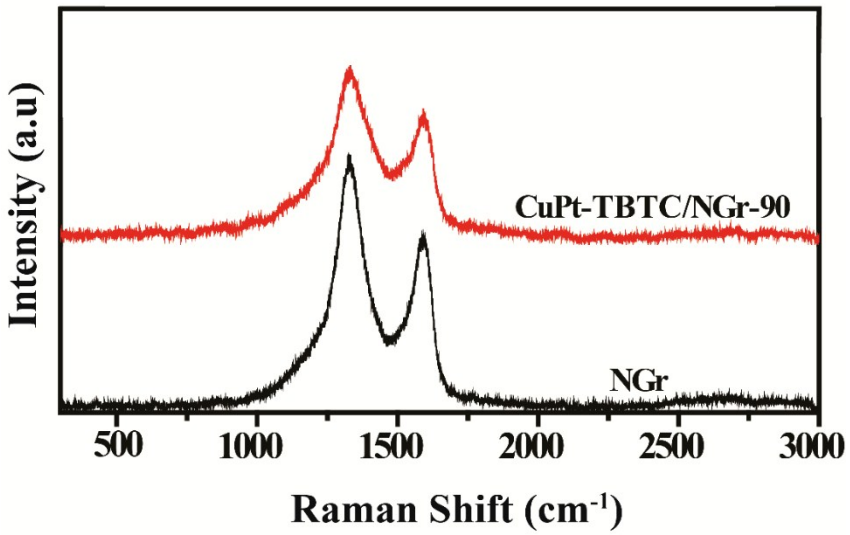

Fig. S10. *Comparative Raman data of NGr and CuPt-TBTC/NGr-90.*

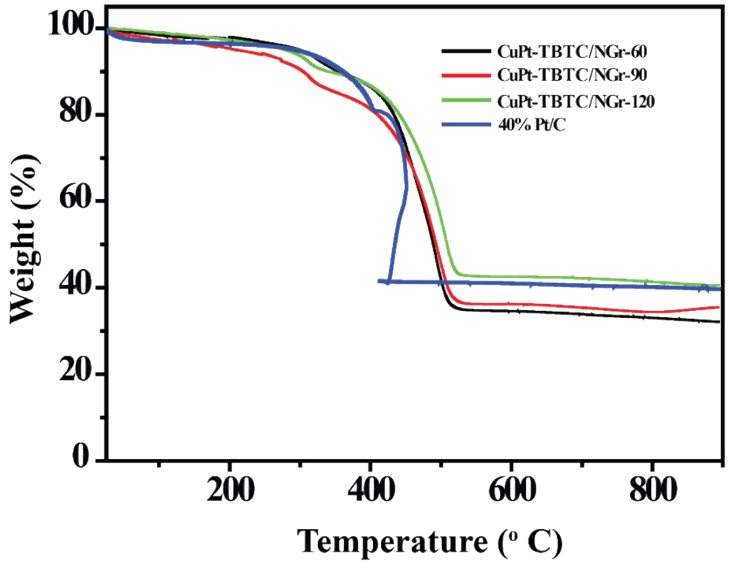

Fig. S11. *TGA profile comparison of CuPt-TBTC/NGr-60, CuPt-TBTC/NGr-90 and CuPt-TBTC/NGr-120 with commercial Pt/C in air atmosphere.*

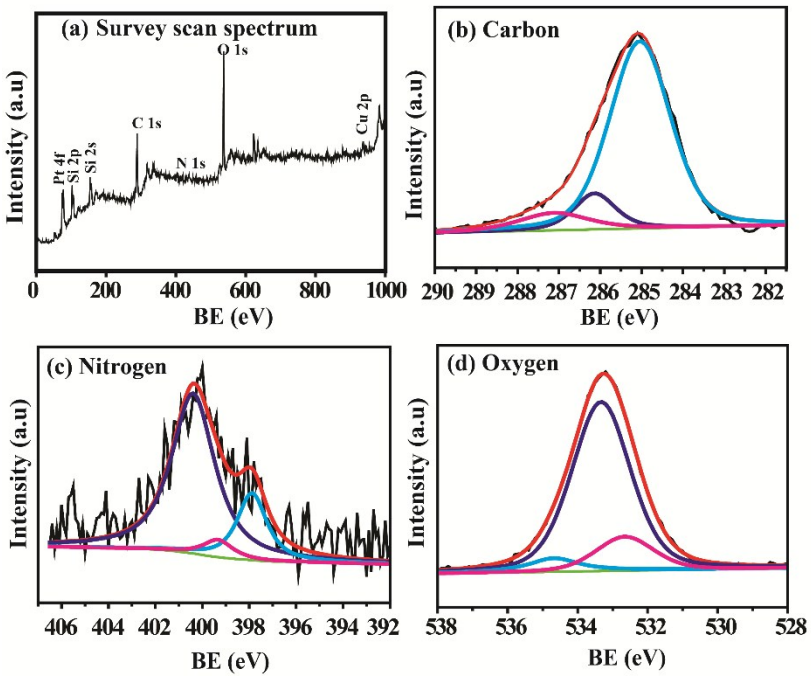

Fig. S12. *(a) XPS survey spectra of CuPt-TBTC/NGr-90, deconvoluted XPS profiles of (b) carbon, (c) nitrogen and (d) oxygen in CuPt-TBTC/NGr-90.*

The presence of Si peak in the XPS survey scan spectrum of CuPt-TBTC/NGr-90 is due to the sample was coated on the Si substrate during the analysis. The presence of oxygen in the survey scan mainly because of the adsorbed oxygen and residual moisture present in the system.

Calculation of Electrochemical Active Surface Area (ECSA)

The ECSA value has been obtained by running the CV in N_2 saturated atmosphere and calculated by using the below equation;

$$ECSA\ (m^2\ g_{pt}^{-1}) = Q_{H\text{-}desorption} / \{0.21 * Pt_{loading}\}$$

where, $Q_{H\text{-}desorption}$ is the charge associated with the hydrogen desorption in mC, 0.21 is the constant charge required to remove the monolayer of adsorbed hydrogen layer and the its unit is mC cm^{-2}, Pt loading for CuPt-TBTC/NGr-90 was 0.014 mg and for Pt/C was 0.02 mg, respectively.

Koutecky-Levich (K-L) equation

The kinetic parameters have been obtained by using the Koutecky-Levich (K-L) equation and it can be represented as;

$$1/j = 1/j_L + 1/j_K \quad \text{---------- (1)}$$

$$1/J = B\omega^{1/2} + 1/j_k \quad \text{---------- (2)}$$

$$\text{where, } B = 0.62\ n\ F\ A\ C_0^*\ D_0^{2/3}\ v^{-1/6}$$

$$\text{and } j_k = n\ F\ A\ k\ C_0^*$$

where, 'j' is the measured current density, 'j_L' is the limiting current density, 'j_k' is the kinetic current density, 'ω' is the angular rotation ($\omega = 2\pi f/60$, f is the rotation speed), 'n' is the number of transferred electrons during ORR, 'F' is the Faraday constant (96480 C), 'C_0^*' is the bulk concentration of O_2 (1.22×10^{-6} mol cm^{-3}), 'D_0' is the diffusion coefficient of O_2 (1.9 x 10-5 $cm^2\ s^{-1}$), 'v' represents the kinematic viscosity of the electrolyte (0.01 $cm^2\ s^{-1}$) and 'k' is the electron transfer rate constant.

The Rotating Ring Disc Electrode (RRDE) technique was used to calculate the number of electron transferred during the ORR process and also to evaluate the H_2O_2 percentage. The

glassy carbon disc (0.2826 cm^2) having a Pt ring was used as the working electrode by keeping the ring potential at 0.6 V, Hg/HgO was used as the reference electrode and a graphite rod was used as the counter electrode. The analysis has been done in the O_2-saturated 0.1M KOH solution. Using the below equation, the number of electron transfer during ORR was calculated:

$$n = \frac{4\,Id}{Id + Ir/N}$$

The H_2O_2 percentage was calculated by applying the formula,

$$H2O2\% = \frac{200 * Ir/N}{Id + Ir/N}$$

where, 'I_r' is the Faradaic ring current, 'I_d' is the Faradaic disc current, 'N' is the collection efficiency (0.37) and 'n' is the number of transferred electrons.

Calibration of the reference electrode

In order to convert the potential from Hg/HgO to RHE, LSV at a scan rate of 1.0 mV/s was carried out in 0.1M KOH solution with saturated hydrogen. Pt was used as the working electrode, Pt wire was as used as the counter electrode and Hg/HgO was used as the reference electrode. The correction factor was chosen as the point at which the current crosses the zero line.

So, E (RHE) = E (Hg/HgO) + 0.870

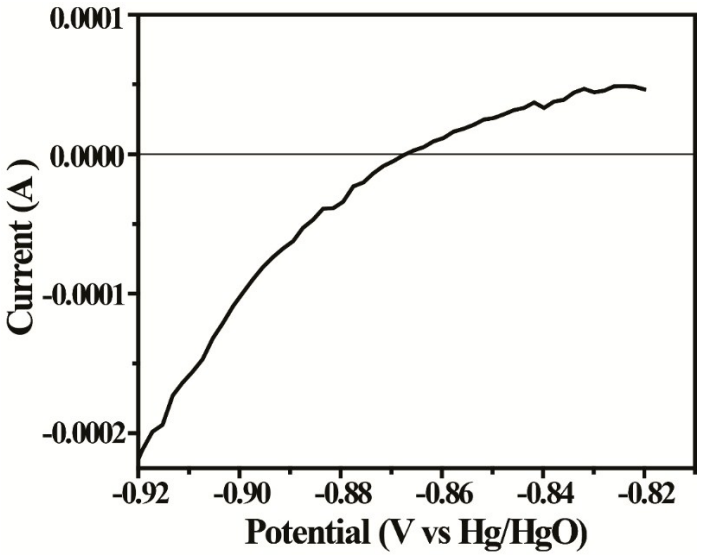

Fig. S13. *Calibration curve for the Hg/HgO reference electrode.*

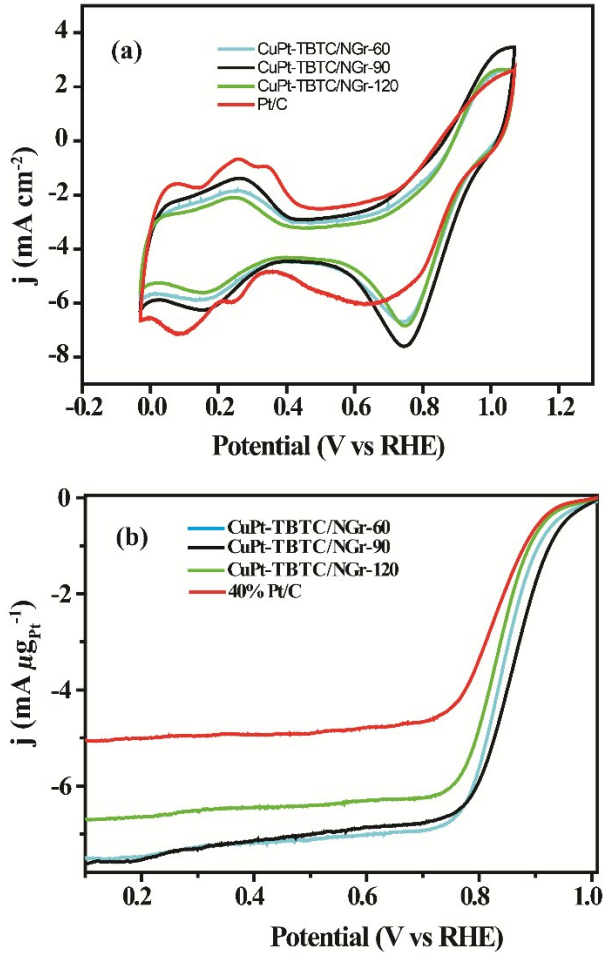

Fig. S14. *(a) Comparative CV profiles recorded at a scan rate of 50 mV sec^{-1} in O_2 saturated 0.1 M KOH and (b) linear sweep voltammogram comparison of CuPt-TBTC/NGr-60, CuPt-TBTC/NGr-90 and CuPt-TBTC/NGr-120 with 40 wt. % Pt/C.*

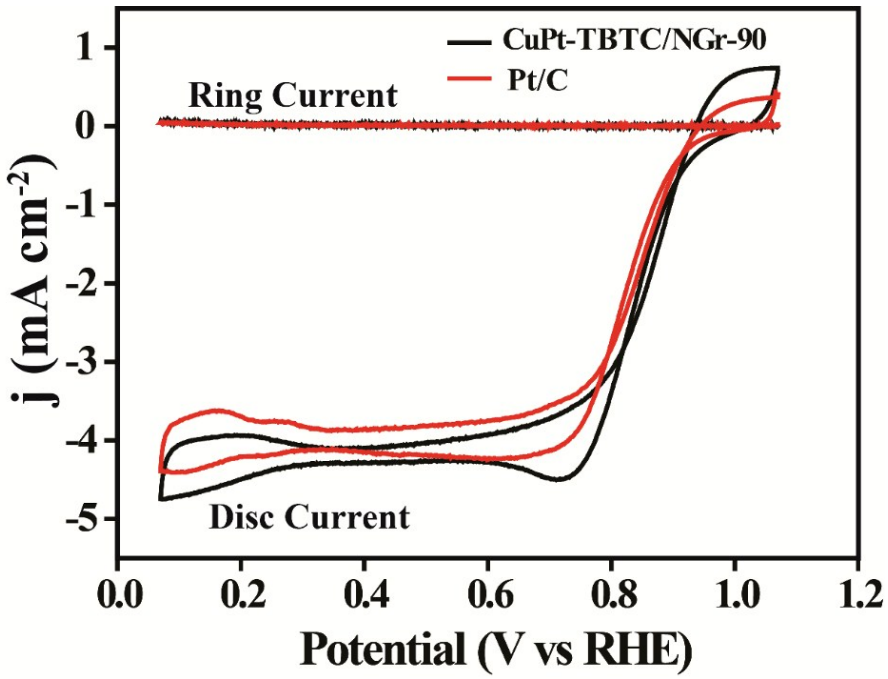

Fig. S15. *Comparison of the RRDE voltammograms of CuPt-TBTC/NGr-90 and 40 wt. % Pt/C.*

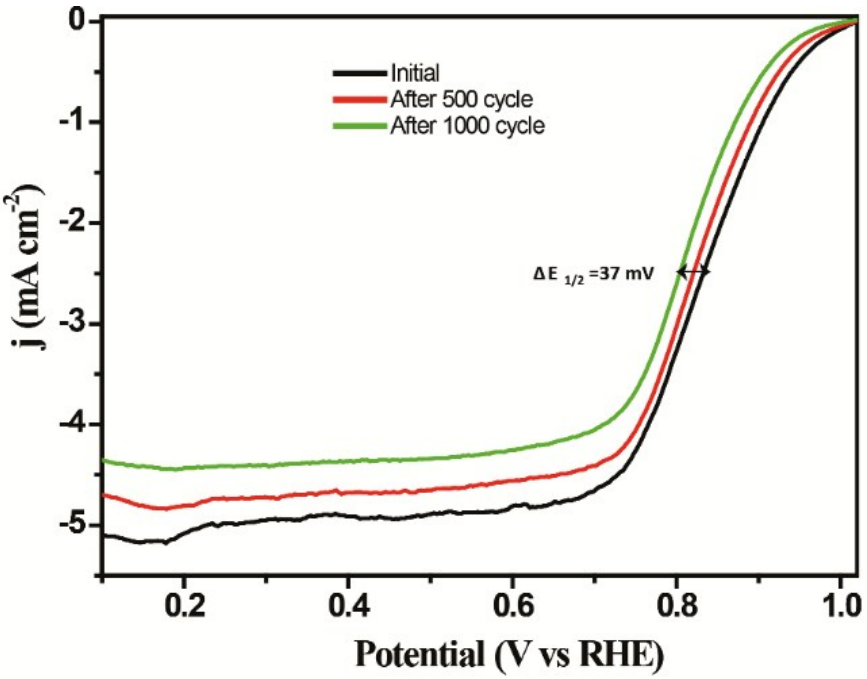

Fig. S16. *Linear sweep voltammograms of 40 wt. % Pt/C before and after the durability study.*

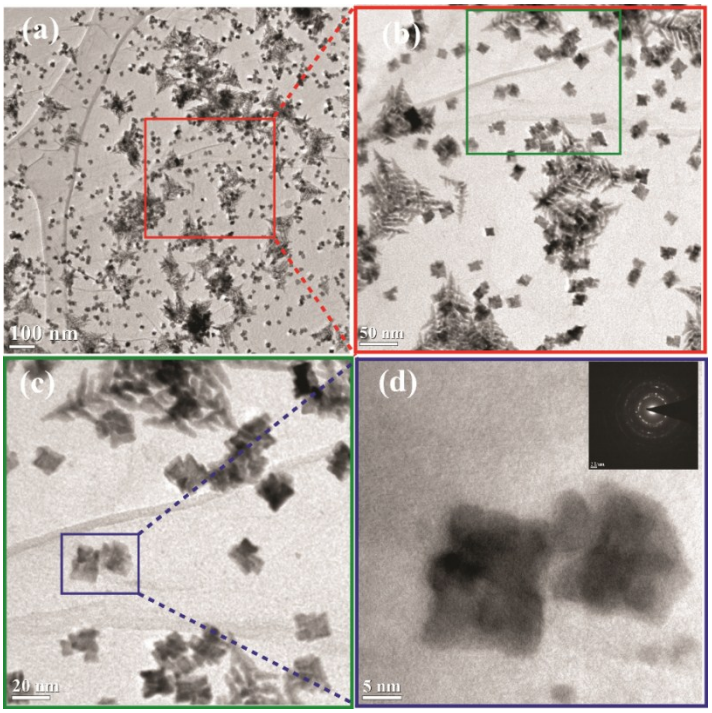

Fig. S17. *TEM images of CuPt-TBTC/NGr-90 recorded after the durability analysis: (a) image indicating the mixed dispersion of the trigonal bipyramidal and truncated cubes on the surface of NGr, (b) higher magnification image of the marked (red) portion of (a) and (c) magnified image of the region marked in the green square in (b) and (d) magnified view of the truncated cube marked in the blue square in (c) with the inset showing the SAED pattern.*